Enhanced Numerical Modeling of Breaking Waves

Final Report for Contract No. N00014-02-C-0431

Prepared for:

The Office of Naval Research

By: Richard Leighton
1200 Joe Hall Drive, P.O. Box 990
Ypsilanti, MI 48197
734-480-5000
Richard.leighton@gd-ais.com

GENERAL DYNAMICS
Advanced Information Systems

September 2006

Report Documentation Page

Form Approved
OMB No. 0704-0188

1. REPORT DATE	2. REPORT TYPE	3. DATES COVERED
SEP 2006	**N/A**	**-**

4. TITLE AND SUBTITLE	5a. CONTRACT NUMBER
Enhanced Numerical Modeling of Breaking Waves	5b. GRANT NUMBER
	5c. PROGRAM ELEMENT NUMBER
6. AUTHOR(S)	5d. PROJECT NUMBER
	5e. TASK NUMBER
	5f. WORK UNIT NUMBER
7. PERFORMING ORGANIZATION NAME(S) AND ADDRESS(ES) **General Dynamics Advanced Information Systems 1200 Joe Hall Drive, P.O. Box 990 Ypsilanti, MI 48197**	8. PERFORMING ORGANIZATION REPORT NUMBER
9. SPONSORING/MONITORING AGENCY NAME(S) AND ADDRESS(ES)	10. SPONSOR/MONITOR'S ACRONYM(S)
	11. SPONSOR/MONITOR'S REPORT NUMBER(S)

12. DISTRIBUTION/AVAILABILITY STATEMENT
Approved for public release, distribution unlimited

13. SUPPLEMENTARY NOTES
The original document contains color images.

14. ABSTRACT

15. SUBJECT TERMS

16. SECURITY CLASSIFICATION OF:			17. LIMITATION OF ABSTRACT	18. NUMBER OF PAGES	19a. NAME OF RESPONSIBLE PERSON
a. REPORT	b. ABSTRACT	c. THIS PAGE			
unclassified	**unclassified**	**unclassified**	**UU**	**14**	

Standard Form 298 (Rev. 8-98)
Prescribed by ANSI Std Z39-18

Contents

List of Figures

Introduction

Hydrodynamic predictions of waves can be made via numerical solution of the Navier–Stokes equations subject to the appropriate free-surface boundary conditions. For practical flow of naval hydrodynamic interest, simplifications to these equations must be made in order to make the computations feasible. Two approaches for this exist: potential flow, where viscous and rotational effects are formally eliminated from the equations, and Reynolds-averaged approaches, where the equations are time-averaged. Potential flow calculations are significantly faster, but cannot account for viscous effects or turbulence. Reynolds-averaged Navier–Stokes (RANS) calculations require significantly more computational effort, as well as turbulence modeling, but constitute a framework which can accommodate both viscous and turbulence effects. The research described herein is motivated by the need for wave breaking models in Reynolds-averaged Navier–Stokes (RANS) calculations.

Although recent developments in level-set and volume-of-fluid numerical methods seem to have relaxed the need for detailed wave-breaking models in the RANS predictions in naval hydrodynamics, the absence of RANS model for breaking waves means some physical processes are not captured. The generation of free-surface roughness and surface currents, the net dissipation of wave energy during breaking or the production of bubbles are examples of processes not captured by standard RANS modeling. Numerical stability (via numerical dissipation) and geometric generality (via surface capturing) alone cannot fully replace the need for models of the unresolved scales, though they will allow for some level of successful calculations.

An approach for developing RANS models for breaking waves can be outlined as follows. Given a particular numerical methodology in a predictive engineering application (VoF, Level set, potential flow, ect.), the choice of which fixes what can be represented in the computation, a complementary averaging (or filtering) process must defined and a new set of 'RANS' equations developed. While the resultant equations may appear the same, the models needed may not be. The unresolved fluid dynamics in a VoF calculation are fundamentally different from the unresolved fluid dynamics in a level-set calculation. Given the 'RANS' equations, the filtering process and the relevant experimental and numerical data, develop the functional form for the model of the unknown terms relevant to breaking and surface roughness. The work herein was intended to provide, when fully executed, data for use in the model development.

Research objectives

The primary goal of this research effort was the development and application of a numerical capability for the simulation of breaking waves including the effects of fluid viscosity, surface tension and the generation of surface roughness and turbulence. The capability sought was to maximize fidelity to the physics of the free-surface, requiring the numerics to predict all relevant scales.

The intent was to develop the ability to both simulate the breaking event and to have a platform in which models could be developed and tested. A fully coupled formulation was adopted in the development of the numerical algorithm. The primary benefits of this approach are the satisfaction of mass conservation and the numerically implicit enforcement of strongly coupled boundary conditions. The algorithm developed is remarkable robust, while maintaining high order of accuracy. The algorithm was implemented in two and three dimensions and several breaking wave simulations were performed. The algorithm was developed to allow both model-free DNS-like calculations and RANS calculations.

An additional objective was to develop an solution scheme which allowed the free-surface to become multiply defined. The intent of this adaptation was not to solve for plunging wave, but rather to simulate the roughness found in less aggressive breaking waves. An appropriate solution to this objective was never achieved.

The algorithm was applied to a variety of conditions, with mixed results. The evolution of small scale two dimensional waves could be followed fully through breaking and into the decay state. Longer, two-dimensional waves have also been simulated, but without sufficiently high resolution, the breaking process is insufficiently dissipative. Many of these two-dimensional simulations become unphysical and fail. Three-dimensional waves were also simulated, but the algorithm was insufficiently vetted to perform the desired full three-dimensional breaking waves.

Approach

The numerical approach adopted for the study of breaking waves was to develop a robust and general solution technique for the Navier-stokes equations including the full non-linear boundary conditions. Since the objective was the development of numerical dataset of simulated breaking waves for use in the development of engineering models, the numerical approach needed to be able fully represent the physics of the breaking waves.

Several approaches were excluded from the list of potential numerical methods. The excluded numerical methods included Level-Set methods, Volume-of-Fluid methods and any approach requiring the linearization of the free surface. While level-set methods can be constructed to be very robust, in general the only satisfy the free-surface boundary conditions in a weak sense. The free surface boundary is represented as a distribution, with compact support, in the vicinity of the mean free surface. As a result, some physical processes may not be fully represented. On the other hand, VoF methods may employ a discrete representation of the fluid volume and a second representation for the interface, such that the union of these grids represents the free surface and the fluid volume. However, the length scales (boundary layer thickness) normal to the air-water interface scales as

$$\delta \sim \mathrm{Re}^{-1/2}, \tag{1}$$

and fully resolving this interface is not practical using the uniformly spaced grid often employed in VoF methods. This does not imply that these methods are not useful in many free-surface problems, but rather they may not capture the physical processes needed in the development of RANS like models for the interface.

The approach adopted was a surface following time dependent structured grid, a high order compact finite difference representation and a Krylov space algorithm for solving the fully coupled Navier-Stokes equations. This representation satisfies the conservation of mass locally and globally on a fully deforming grid. The primary limitation of this approach, aside from computationally efficiency, is the inability to generate usable grids when the surface slope exceed vertical.

Governing Equations

Navier-Stokes (RANS) governing equations are:

$$\nabla \cdot \mathbf{u} = 0 \tag{2}$$

$$\frac{\partial \mathbf{u}}{\partial t} + \frac{1}{2}\left((\mathbf{u}\cdot\nabla)\mathbf{u} + \nabla\cdot(\mathbf{uu})\right) = -\nabla(p + gy) + \nabla\cdot\left((\nu + \nu_e)\nabla\mathbf{u}\right) + \mathbf{F_b} \tag{3}$$

where $\mathbf{F_b}$ is an body force used to model the forcing of submerged foils and ν_e is an eddy viscosity, employed as needed. Note the hydrostatic pressure is retained in the governing equations, rather than being included in the boundary condition. Boundary conditions imposed on the free surface are the kinematic boundary condition

$$\frac{\partial \eta}{\partial t} + \mathbf{u}\cdot\nabla\eta = v \qquad \text{on} \quad y = \eta(x,z,t), \tag{4}$$

and the dynamic boundary conditions

$$\begin{aligned} \mathbf{n}\cdot\boldsymbol{\sigma}\cdot\mathbf{n}^T &= -P_a - \tfrac{1}{We}\nabla\cdot\mathbf{n} \\ \mathbf{t_x}\cdot\boldsymbol{\sigma}\cdot\mathbf{n}^T &= \mathbf{t_x}\cdot\boldsymbol{\tau_a} \\ \mathbf{t_z}\cdot\boldsymbol{\sigma}\cdot\mathbf{n}^T &= \mathbf{t_z}\cdot\boldsymbol{\tau_a} \end{aligned} \quad . \tag{5}$$

where P_a and τ_a are the normal and shear stress imposed by the atmosphere. $\mathbf{n}_a$, $\mathbf{t}_x$ and $\mathbf{t}_z$ are the free surface normal and tangential vectors , respectively, and $\boldsymbol{\sigma}$ is the stress tensor:

$$\boldsymbol{\sigma} = -p\mathbf{I} + \tfrac{1}{2}\left(\nabla\mathbf{u} + (\nabla\mathbf{u})^T\right).$$

Either shear-free and no-slip boundary conditions can be employed on the bottom of the domain which may be an arbitrary shape.

Numerical Approach

The time stepping algorithm is a mild modification to the common Adams-Bashforth/Crank-Nicholson scheme. In such a scheme, the convective terms as advanced in time explicitly by an Adams-Bashforth representation. The linear, but coupled viscous and pressure terms in the NSE are advanced implicitly with the Crank-Nicholson scheme. While the Crank-Nicholson scheme is unconditionally stable for viscous flows, as the Reynolds number increases, the pressure field will develop a 'checker board instability' in time. Therefore to prevent the formation of the temporal instability, the Crank-Nicholson scheme is replace by the so-called theta scheme:

$$\left.\frac{df}{dt}\right|_n \cong \frac{\theta f_n + (1-\theta) f_{n-1}}{\Delta t},$$

where $0 < \theta < 1$. When $\theta = 0.5$, the scheme is standard Crank-Nicholson, while in this work a value of $\theta = 0.51$, was usually sufficient to prevent oscillations in time. For simplicity, the description of the time advancement scheme assumes the Crank-Nicholson scheme

The outline of the time advancements algorithm is as follows:

$$\begin{aligned} \mathbf{u}^{n} + \tfrac{\delta t}{2}[\nabla p]^{n} - \tfrac{\delta t}{2}\left[\nabla\cdot\left((\nu+\nu_{e})\nabla\mathbf{u}\right)\right]^{n} &= \mathbf{u}^{n-1} + \tfrac{\delta t}{2}[\nabla p]^{n-1} - \tfrac{\delta t}{2}\left[\nabla\cdot\left((\nu+\nu_{e})\nabla\mathbf{u}\right)\right]^{n-1} \\ &\quad + \delta t\left[\left(\tfrac{3}{2}\mathbf{N}^{n-1} - \tfrac{1}{2}\mathbf{N}^{n-2}\right) + (\mathbf{F_b} - g\mathbf{e}_2)\right] \\ \nabla\cdot\mathbf{u}^{n} &= 0 \\ \eta^{n} + \frac{\delta t}{2}\hat{u}\left[\frac{\partial\eta}{\partial x}\right]^{n} - \tfrac{\delta t}{2}v^{n} &= \eta^{n-1} + \tfrac{\delta t}{2}v^{n-1} - \frac{\delta t}{2}\hat{u}\left[\frac{\partial\eta}{\partial x}\right]^{n-1} \end{aligned} \quad . \qquad (6)$$

where

$$\mathbf{N} = \frac{1}{2}\left((\mathbf{u}\cdot\nabla)\mathbf{u} + \nabla\cdot(\mathbf{u}\mathbf{u})\right)$$

is the nonlinear term, and $\hat{u}$ is an extrapolated value of the surface velocity at forward half step in time. The computations are performed in the physical domain or grid (the velocities remain the usual Cartesian velocities), but the derivative are all evaluated on an orthogonal computational grid. The mapping between the physical grid and computational grid, represented by the metrics is general and grid motion is fully accounted for.

Collectively these equations are a set of 3 2-D plus 1 1-D coupled equations in two dimensions or 4 3-D plus 1 2-D coupled equations in three dimensions. These equations can be written formally as

$$\begin{bmatrix} A_{\mathbf{u}}^{n+1} & G^{n+1} & B_{\eta}^{n+1} \\ D^{n+1} & 0 & 0 \\ E^{n+1} & 0 & A_{\eta}^{n+1} \end{bmatrix} \begin{bmatrix} \mathbf{u}^{n+1} \\ p^{n+1} \\ \eta^{n+1} \end{bmatrix} = \begin{bmatrix} \mathbf{r}_{u}^{n} \\ 0 \\ r_{\eta}^{n} \end{bmatrix} + \begin{bmatrix} \mathbf{b}_{u}^{n} \\ 0 \\ b_{\eta}^{n} \end{bmatrix}. \qquad (7)$$

The first row represents the momentum equation and the second is the continuity equation. The third row is the free-surface kinematic boundary condition. Most of the entries in the left hand side are self-evident, but two are worthy of note. In the top row, B_{η}^{n+1} represents the coupling of the free-surface elevation into the free-surface dynamic boundary conditions, while in the third row, E^{n+1}, is the coupling the surface velocity into the kinematic free surface boundary condition. The metrics are included in the terms of the matrix, which must be updated each time step since the grid metrics are time dependent.

The common approach in solving the incompressible Navier-Stokes equations is to decompose or split them into two or more sequential processes or operators. The operator splitting is done to decouple the viscous and convective processes from the calculation of the pressure and enforcement of continuity. While robust algorithms can be developed by employing splitting, when operator split algorithms are used in Direct Numerical Simulations, the continuity constraint may not be completely satisfied at the

boundaries. Furthermore, the coupling exhibited in the free-surface boundary conditions cannot be handled consistently in a split algorithm.

The alternate and adopted approach is to retain the fully coupled system of equations, and implementing an algorithm which allows the satisfaction of the boundary conditions and the continuity constraint in a numerically semi-implicit form time stepping algorithm. This coupled set of algebraic equations must be solved at each time step. To keep the problem manageable, an algorithm, which does not require the explicit construction of the algebraic system is necessary.

A matrix free pre-conditioned bi-conjugate gradient scheme (BiCGstab) was employed to solve the system of equations. The BiCGstab schemes have been shown effective in algebraic systems which are strongly asymmetric and not positive definite, as long as an appropriate pre-conditioner can be developed. To be effective in this calculation, the pre-conditioner, which is a computationally inexpensive approximation to the system above, must act as a regularizing process. An incomplete Uzawa-scheme was used as the preconditioner. The Uzawa scheme is essentially an approximate LU matrix decomposition of the equation (7). The incomplete LU decomposition as applied to the equation above is similar to the operator splitting scheme noted above. The preconditioner is applied, in parallel, on the decomposed domain. The BiCGstab algorithm provides the global coupling.

For sufficiently smooth grid, such as that in Figure 1, the iteration scheme forces the residual of equation (7) to ~10^{-13} in 150 to 250 iterations. Even for very ill-constructed unsmooth grid, such as those observed when the simulated breaking event becomes unphysical, the numerical scheme will continue to converge, albiet slowly, to a (unphysical) solution. While computing unphysical solution is the objective, a robust solution technique was required.

Geometry and Grid Generation

The formulation of the grid-transformed equations, described above, is completely general. The computational grid is not required to be orthogonal within the domain or at the free surface. The grid may include a multiply defined free-surface. The only limitation as formulated was that the domain by simply connected: re-entrant breaking waves wherein enclosed air cavities occur are excluded. Although surface following algorithms may best predicted capillarity dominated wave physics, are ill-suited for re-entrant wave breaking. An objective of the research was to develop a grid generation scheme allowing for multiply defined surfaces. This objective was to address the occurrence of highly contorted surfaces where in the slope may exceed vertical, but not include reentrant flows, but a satisfactory method of generate a smooth grid for the multiply defined geometry was never developed

The waves to be simulated were assumed from the start to exist in a periodic domain so that the emphasis could be placed on the development of the numerical method. Two approaches for grid generation were considered: algebraic grid generation and hyperbolic grid generation. For sufficiently benign free-surfaces the hyperbolic grids were acceptable, though more costly than simple algebraic grids. However generating a smooth hyperbolic grid when the free-surface becomes sufficiently distorted is difficult. The easier, though more restrictive, approach was to use algebraic grid generation. The algebraic grids are intrinsically smoother and resulted in better convergence. The algebraic grids were generated via a spline technique, which allows for easy adjustment to keep the grid nearly orthogonal the free surface. Figure 1 displays an example of the streamwise velocity of an artificially steep wave $(k\alpha = 1,\ \lambda = 1\mathrm{m})$, along with the grid.

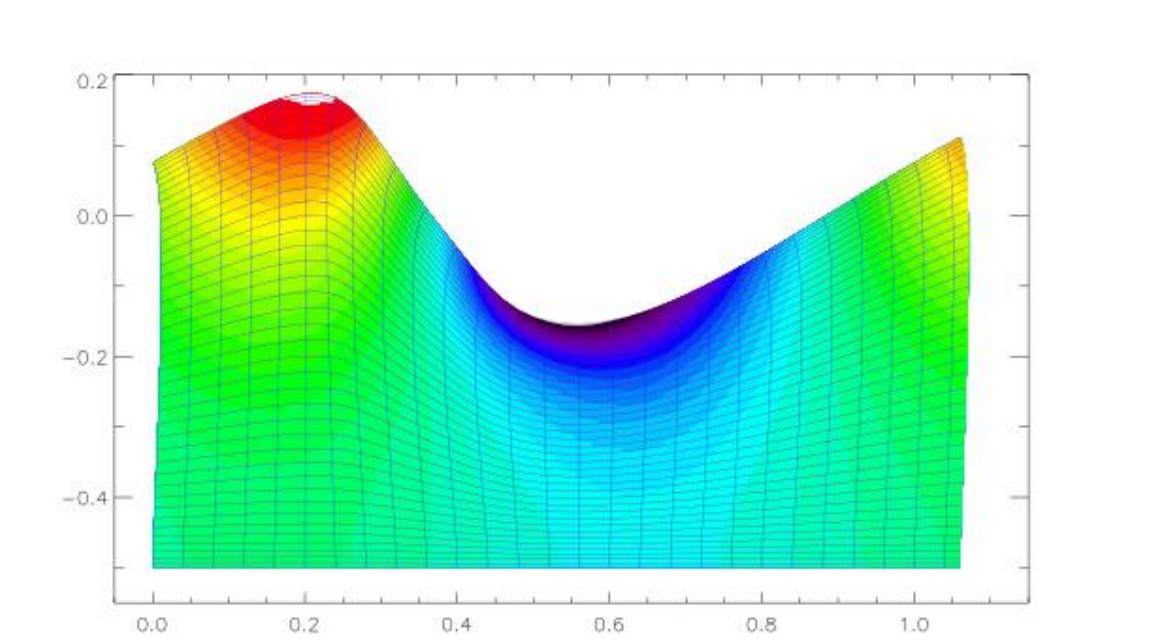

Figure 1 Sample wave calculation showing streamwise velocity and deforming grid.

Figure 2 displays the streamwise velocity over a shear free hump, along with an instance of the grid. The (periodic) channel is a meter long and 10 cm deep. The objective was to examine and model the production of turbulence in a breaking zone, modeled as a hydraulic jump. A multiblock boundary exists at y = 0.5. As the computation proceeded, the face of the hydraulic jump approach vertical and the calculation failed. Mass was conserved during the calculation.

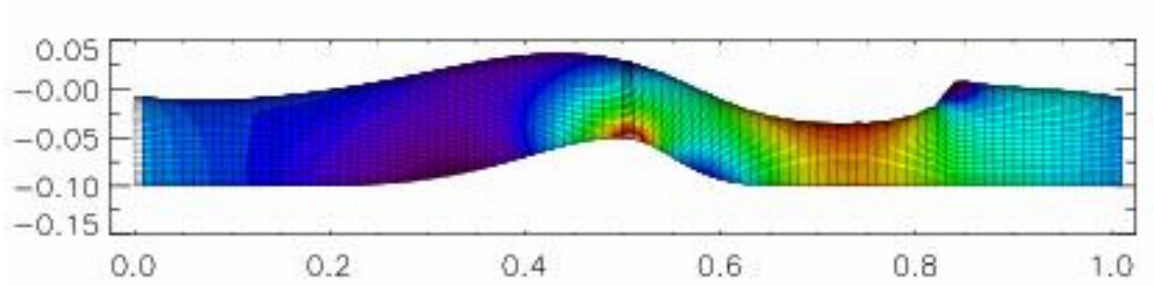

Figure 2. Streamwise velocity, flowing to the right, over a shear-free hump. Mean velocity is 0.5 m/s. Slow velocity is purple, faster velocities are red.

As implied above, the domain was decomposed in several block and a parallel algorithm was implemented using the MPI standard.

Extensions

Two extensions to the two dimensional algorithm were to be implemented. As the calculations proceeded, turbulence models were to be implemented. These turbulence models were to enhance the

dissipation of wave energy and control the breaking process. The second extension was to implement the algorithm in three dimensions.

Turbulence Modeling

Two types of turbulence models were implemented: a simple Smagorinsky type LES model and the standard k-ε two equation model. The former was a simple add-on sometimes used in initializing the code. The two-equation model was exercised, but never thoroughly vetted. The primary missing element in the model was a term to initiate the production of turbulence kinetic energy when the spilling starts. Several were considered based on the local surface compression on the face of the wave, but none were successfully developed in the time allocated.

Extension to Three Dimensions

The algorithm was also implemented in three dimensions. The 3-D code exhibits the same iterative convergence characteristics as its two-dimensional counterpart. The code retains all the same grid issues and numerical approaches as the two-dimensional version. Some limited results will be presented below (See Figure 6.)

The code was not sufficiently vetted before the end of the contract to effectively use the HPC resources available at the time and is too computationally intensive for the currently available resources. Tuning the inter-process communication was accomplished for the two dimensional application, but remained inefficient in the three-dimensional code.

Two Dimensional Calculations

The role of the two-dimensional calculations was for validation and optimization of the algorithm in the limit of strong small scale dynamics. While these simulations may be of questionable utility in the context of naval hydrodynamics, they are a necessary step towards developing tools for predicting the larger scale breaking.

'Wind Driven' Breaking

A set of small scale breaking wave simulations, referred to as wind driven, were performed for the purpose of (1) understanding the limits and limitations of the algorithm, (2) testing and optimizing the computer code and (3) to provide insight into the process by which turbulence and surface roughness are generated. These simulations calculate the evolution of an initially linear wave driven to breaking by a phase-locked external 'atmospheric' pressure. Such a calculation is presented in Figures 3-5, wherein a small-scale wave is driven past breaking. In Figure 3, the vorticity is generated at the interface near x=0.625. The source of the vorticity is driven downstream by the wave propagation and as expected a packet of resonant capillary waves are observed ahead of this point. (The decaying vortex seen upstream is a consequence of the periodic domain.) The vorticity is unsteady, rolling up into nearly discrete vortices. However, the generation of vorticity occurs predominately at the localized source.

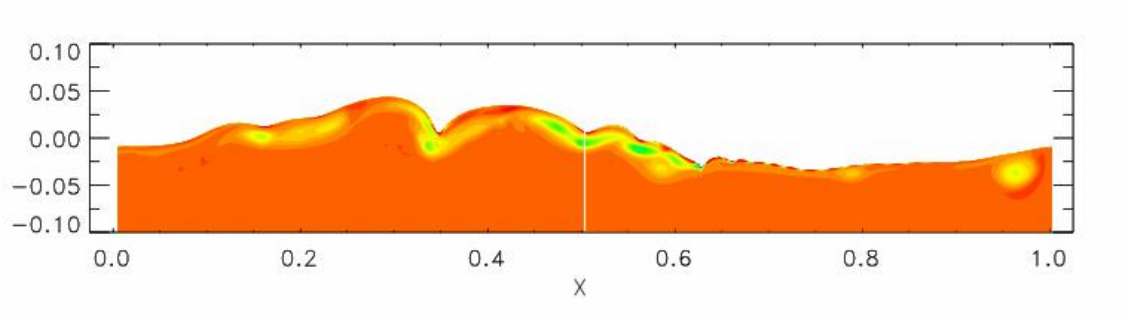

Figure 3 Tangential vorticity in late breaking of a 10 cm wave. The vorticity ranges from -3250 sec-1 to 3750 sec-1. The frequency of the wave is approximately 25 rad sec-1. The vertical bar at x=0.5 indicates the block boundary.

The surface elevation characteristics of this wave are presented in Figure 4. The salient features are (1) the strong depression, and resulting curvature near x=0.35 and (2) the strong, but compact, negative peak in curvature at the source vorticity. The magnitude of the instantaneous slopes can exceed unity.

The complicated interaction of the compact vorticity and the strong depressions like that occurring at x=0.35 may be a process by which air is entrained at the interface. When simulations of this type are performed at lower resolution, these interaction are not as intense. With increasing resolution, these cavities have been observed to grow. Due to grid limitations, these cavities cannot pinch off and the growth leads to unphysical results. To prevent the uncontrolled growth of these cavities, a special sixth-order filter is applied to the surface elevation.

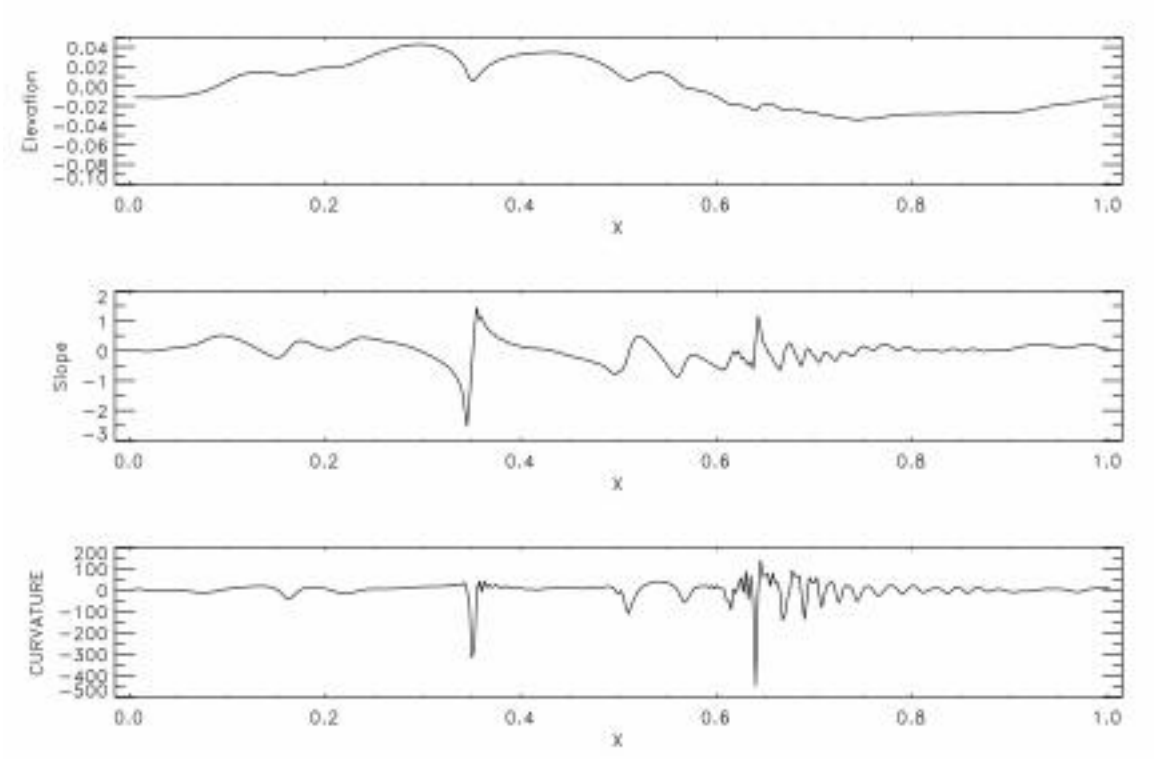

Figure 4 Surface elevation, slope and curvature of wave in Figure 3.

The plot of the curvature in Figure 4, exhibits small wiggles, which are probably erroneous. Once the wiggles are created, real or otherwise, they propagate like capillary waves, with a phase speed proportional to the reciprocal of the square root of their wavelength. Simulating these small capillary waves requires an implicit numerical scheme to reduce the time stepping constraint in explicit schemes.

A final observation relevant to the development of wave breaking models can be made. In Figure 5, the fluid velocity at the surface is resolved into the surface normal and tangential directions. Note the strong negative rate-of-strain where the vorticity is generated, while the rate-of-strain has a dipole character near the depression. As a result the will be a flux of vorticity into the fluid in the former case, but not in the later case. This observation is important in the context of the development of RANS models for breaking waves. In addition to providing some unsteadiness, this region for the production or flux of vorticity creates the shear-layer riding on the face of the breaking wave.

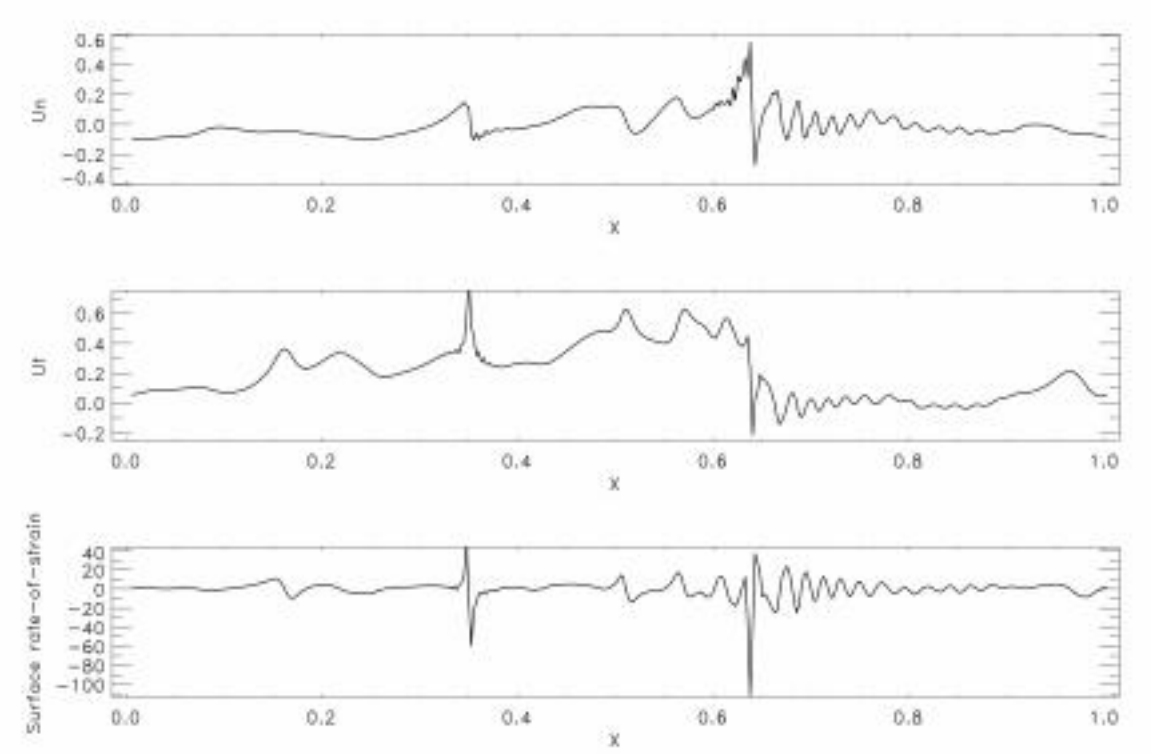

Figure 5. Fluid velocity at surface of the wave in Figure 3 resolved into surface normal and tangential components. . For comparison, the phase velocity of the linear wave in these non-dimensional units is approximately 0.4. The surface rate-of-strain in the bottom frame.

Three-Dimensional Calculations

A preliminary and limited set of three-dimensional wave simulations for the purpose of testing and validating the code were performed. Two geometries were considered: interacting oblique waves and recirculating open channel flow with a bottom bump. These cases validated the general extension of the numerics to three dimensions. Additionally, the inter-block communications used in the domain decomposition were tested and validated.

A sample calculation of recirculating flow over a shear free hump is shown in Figure 6 & 7. This computational domain consists of six blocks. The three frames showing unsteady pressure in Figure 6 are separated in time by the H/U where H is the channel depth and U is the mean velocity. Figure 7 is the streamwise velocity at the last frame. The pressure field drops rapidly behind the bump resulting in a strong surface depression. As a result of Bernoulli's law, the velocity above the hump is also increased. As the calculation proceeds, the flow attempts to develop a hydraulic jump, but the simulation was never performed with sufficient resolution.

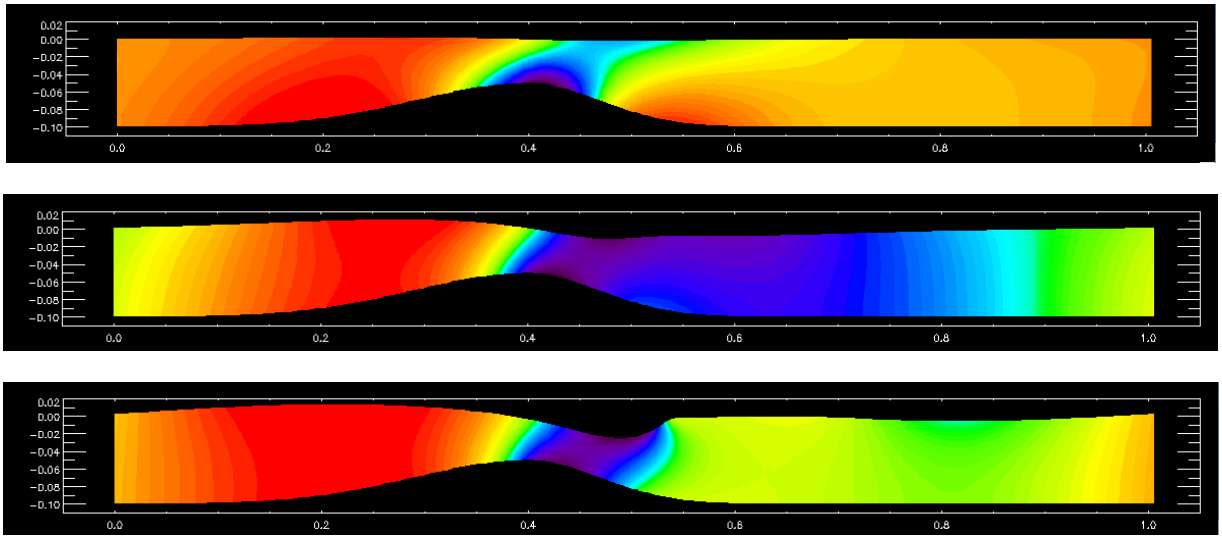

Figure 6. The unsteady pressure in a recirculating channel. The frames are separated by H/U in time.

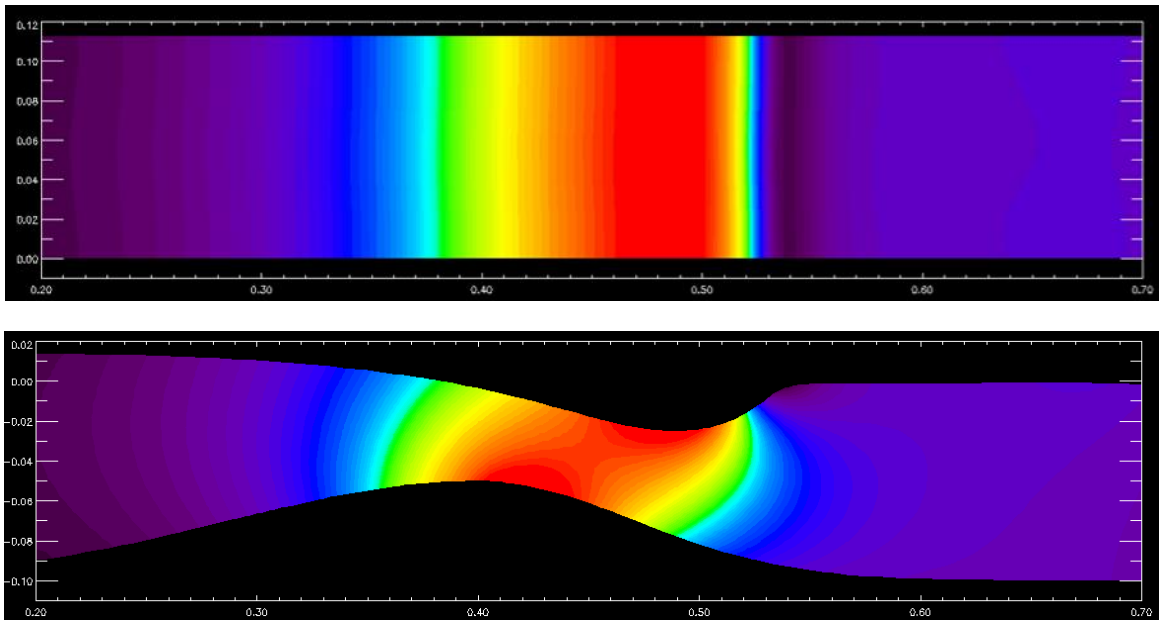

Figure 7.. Streamwise flow over shear-free hump. Flow is to the right.

Summary

The primary objectives were the development and application of the capability to simulated breaking waves. This was seen as part of the larger and longer term objective of developing RANS models for the effects breaking waves.

Algorithms were developed for simulating waves in two and three dimensions. To a limited extent these computer codes are capable of meeting the objective of simulating breaking waves. The numerical algorithms are robust in both two and three dimension, but critical limitations remain.

In two-dimensions, small scale unsteady breaking was simulated. The development of surface roughness and the possible entrainment of air were observed. In some strongly forced open channel simulations, the surface could become sufficiently energetic that possible fluid ejection was observed. With increase wavelength, the restraining influence of surface tension was reduced and the simulations become more difficult. This is more the result of the limited grid implementation, than in the algorithm itself.

A similar algorithm was implemented in three-dimensions, but insufficient time was allocated to its development and validation. While the capabilities are the same as its two-dimensional counter part, substantially greater resources are required.